

Anisotropic magnetoresistance of Co-Pd alloys

S. U. Jen*

Institute of Physics, Academia Sinica, Taipei, Taiwan, Republic of China

(Received 19 August 1991)

The anisotropic magnetoresistance $\Delta\rho/\rho_0$ and electrical resistivity ρ_0 of $\text{Co}_{100-x}\text{Pd}_x$ alloys were measured at $T=4, 77,$ and 300 K. The temperature dependence of $\Delta\rho/\rho_0$ is used to yield $(\Delta\rho/\rho_0)_{\text{imp}}$ and $(\Delta\rho/\rho_0)_{\text{ph}}$ data for Co-Pd alloys as a function of x . A two-current model and theories based on extended versions of it are used to explain the spin-down resistivity ρ^\downarrow and spin-up resistivity ρ^\uparrow . There exists a maximum in ρ^\downarrow at $x=65$ at. % Pd. For $x \geq 50-75$ at. % Pd, $\rho_{sd}^\downarrow \neq 0$ due to the magnetic weakness for the spin-up d band. ρ_{ss} follows Nordheim's rule, and ρ_{ss} increases, going from the Co-Ni to the Co-Pd case.

I. INTRODUCTION

The two-current model of Campbell, Fert, and Jaoul^{1,2} has been successful in accounting for the anisotropic magnetoresistance $\Delta\rho/\rho_0$ in most nickel-rich crystalline alloys. In short, this model states that, at $T \approx 0$,

$$\Delta\rho/\rho_0 = \gamma(\rho^\downarrow/\rho^\uparrow - 1), \quad (1)$$

where ρ^\downarrow and ρ^\uparrow are the resistivities for the spin-down and -up bands, respectively, and $\gamma \approx 0.01$. The condition $\rho^\downarrow/\rho^\uparrow \gg 1$ is assumed. In order to extend the theory to structurally disordered or weakly ferromagnetic materials, Malozemoff has given a more general formula,³ which may be given as follows:

$$\Delta\rho/\rho_0 = \gamma \frac{(\rho_{sd}^\downarrow - \rho_{sd}^\uparrow)(\rho_{sd}^\downarrow + \rho_{ss}^\downarrow - \rho_{sd}^\uparrow - \rho_{ss}^\uparrow)}{(\rho_{sd}^\downarrow + \rho_{ss}^\downarrow)(\rho_{sd}^\uparrow + \rho_{ss}^\uparrow)}, \quad (2)$$

where ρ_{ss}^\downarrow and ρ_{sd}^\downarrow are the resistivities arising from the s - s and s - d scatterings, respectively, in spin-down bands. ρ_{ss}^\uparrow and ρ_{sd}^\uparrow are the resistivities from the corresponding scatterings in spin-up bands. Finally, to extend the theory to the region of concentrated alloys, Berger has discussed the case in which the scattering potential with alloy disorder is strong.⁴ The limitation of his approach is that both γ and r_F are assumed to be independent of the alloy composition x . $r_F \equiv |C_A(\epsilon = \epsilon_F)/C_B(\epsilon = \epsilon_F)|^2$, where $A = \text{Co}$ and $B = \text{Pd}$. C_A or C_B is the average of the coefficient $C_{ln}(\epsilon)$, used in the tight-binding approximation, over the atom A (Co) or B (Pd).

In this paper we will mainly discuss the anisotropic magnetoresistance of $\text{Co}_{100-x}\text{Pd}_x$ alloys. The magnetic and electrical resistivity properties for this same series of Co-Pd alloys have been studied previously.⁵ In Ref. 5 we find that, for $\text{Co}_5\text{Pd}_{95}$, $\alpha \equiv \rho^\downarrow/\rho^\uparrow \approx 2$. Although, as discussed in Ref. 5, the localized picture is expected to be applicable, we nonetheless choose a band picture to explain our results. The main reason is that as x decreases from 95 at. %, the band model becomes increasingly more appropriate. Here we just use the $\Delta\rho/\rho_0$ and α

data of $\text{Co}_5\text{Pd}_{95}$ to extract the value of γ , which is usually a parameter known only to an order of magnitude. In addition, we will show that even if we use a different γ , our main conclusion in this paper will be unaffected.

One problem in this approach has already been encountered in Ref. 5: In the treatment of the temperature dependence of the resistivity $\text{Co}_5\text{Pd}_{95}$, there is a complication resulting from paramagnon scattering;⁶ i.e., for $T < T_{sf}$, the ideal resistivity ρ_T of the alloy is proportional to T^2 , but for $T > T_{sf}$, the behavior $\rho_T \propto T$ may result. For Pd-rich alloys, $T_{sf} \equiv 0.25T_s \approx 20$ K. Perhaps the paramagnon theory can explain why in Ref. 5 we observed an anomalously large coefficient for the T^2 term in ρ_T for $T \leq 20$ K. But more significant is the fact that in Ref. 5 we took another temperature range, $20 < T < 50$ K, for the fitting, in which only the T^2 and T^3 dependences are evident, to obtain α . In the $20 < T < 50$ K region, there is little or no T dependence as predicted from paramagnon-scattering theory. Moreover, since, in Ref. 5, $\alpha \approx 2$ is also obtained by another method, independent of the temperature effect, the same α value is used here for purposes of discussion.

II. EXPERIMENTS

The details of $\text{Co}_{100-x}\text{Pd}_x$ sample preparation were described before.⁵ The anisotropic-magnetoresistance measurements are performed with standard techniques. We used a CF1200 liquid-helium cryostat and an ITC4 temperature controller, both made by Oxford Instrument, to maintain the sample temperature. We made measurements at three fixed temperatures $T=4, 77,$ and 300 K. The temperature stability was good to within ± 0.2 K. A 7-in. electromagnet produced external fields up to 1 T. The sample is aligned either parallel or perpendicular to the field to measure ρ_{\parallel} or ρ_{\perp} . Characteristic ρ_{\parallel} and ρ_{\perp} at 4 K for $\text{Co}_{45}\text{Pd}_{55}$ crystalline alloys are shown in Fig. 1. The anisotropic magnetoresistance is defined as

$$\Delta\rho/\rho_0 = (\rho_{\parallel}^s - \rho_{\perp}^s) / (\frac{2}{3}\rho_{\parallel}^s + \frac{1}{3}\rho_{\perp}^s),$$

where ρ_{\parallel}^s and ρ_{\perp}^s are the saturated resistivities of ρ_{\parallel} and ρ_{\perp} .

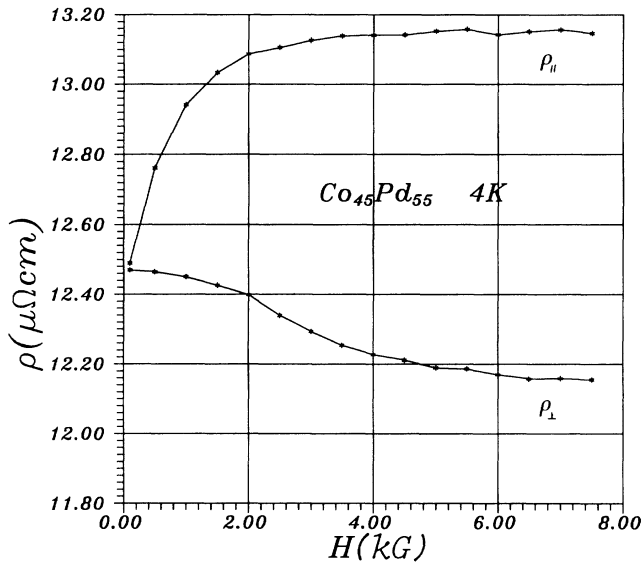


FIG. 1. Anisotropic resistivities ρ_{\parallel} in parallel fields and ρ_{\perp} in perpendicular fields of $\text{Co}_{45}\text{Pd}_{55}$ at $T=4\text{K}$.

III. TEMPERATURE DEPENDENCE OF $\Delta\rho/\rho_0$ IN Co-Pd

According to theory,^{7,8} if $\alpha \gg 1$, Matthiessen's rule can be used to derive the temperature dependence of $\Delta\rho/\rho_0$:

$$\frac{\Delta\rho}{\rho_0}(T) = \left[\frac{\Delta\rho}{\rho_0} \right]_{\text{ph}} + \left[\left[\frac{\Delta\rho}{\rho_0} \right]_{\text{imp}} - \left[\frac{\Delta\rho}{\rho_0} \right]_{\text{ph}} \right] \frac{\rho_0(4.2\text{K})}{\rho_0(T)}, \quad (3)$$

where $\rho_{\parallel}(T) = (\rho_{\text{imp}} + \rho_{\text{ph}})_{\parallel}$, $\rho_{\perp}(T) = (\rho_{\text{imp}} + \rho_{\text{ph}})_{\perp}$, and $\rho(4.2\text{K}) \approx \rho_{\text{imp}}$.

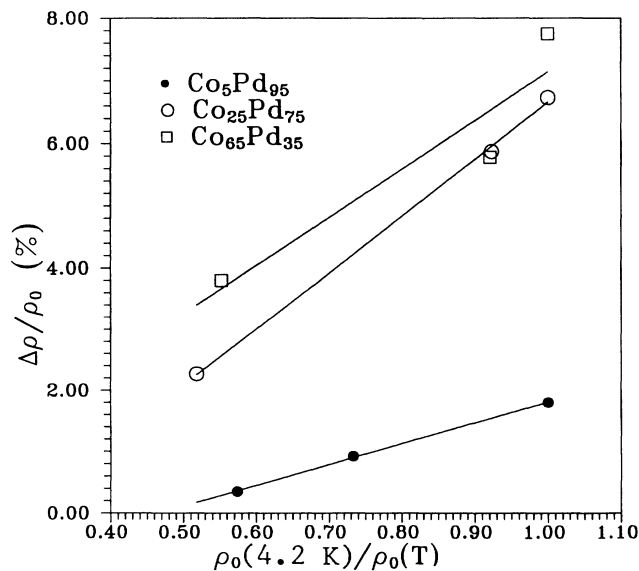


FIG. 2. Fittings of $\Delta\rho/\rho_0$ as a function of $\rho_0(4.2\text{K})/\rho_0(T)$ with Eq. (3) for $\text{Co}_5\text{Pd}_{95}$, $\text{Co}_{25}\text{Pd}_{75}$, and $\text{Co}_{65}\text{Pd}_{35}$ alloys.

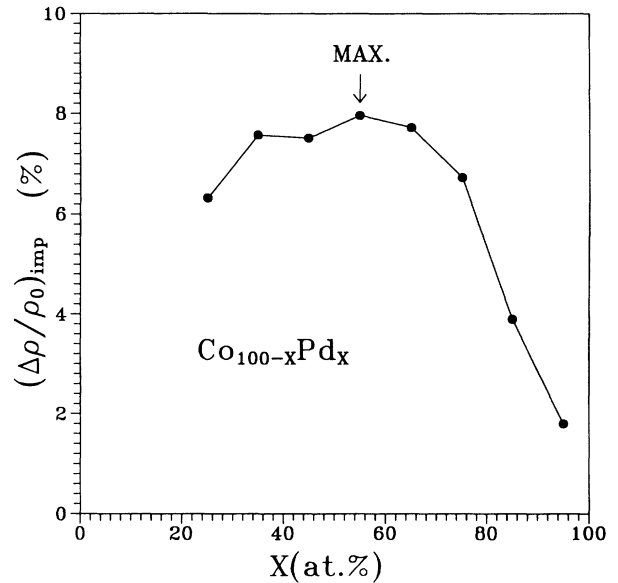


FIG. 3. $(\Delta\rho/\rho_0)_{\text{imp}}$ is defined as $(\Delta\rho/\rho_0)$ at $T=4\text{K}$; $(\Delta\rho/\rho_0)_{\text{imp}}$ is plotted for each Pd concentration x .

For Co-Pd alloys, the condition $\alpha \gg 1$ is not as strictly satisfied as for Co-Ni, Ni-Fe, and Ni-Mn alloys. As will be discussed later, the α of concentrated Co-Pd is about 5. Hence Eq. (3) is considered here as an empirical formula for obtaining $(\Delta\rho/\rho_0)_{\text{imp}}$ and $(\Delta\rho/\rho_0)_{\text{ph}}$ for Co-Pd alloys. Figure 2 shows the fitting of $\Delta\rho/\rho_0$ of $\text{Co}_5\text{Pd}_{95}$, $\text{Co}_{25}\text{Pd}_{75}$, and $\text{Co}_{65}\text{Pd}_{35}$ versus $\rho_0(4.2\text{K})/\rho_0(T)$ at three temperatures $T=4, 77,$ and 300K . From the diagram the linear fit of Eq. (3) seems pretty good. By extrapolating each line to the vertical axis where $\rho_0(4.2\text{K})/\rho_0(T)=0$, we can determine $(\Delta\rho/\rho_0)_{\text{ph}}$. On the lowest-temperature side, we use $(\Delta\rho/\rho_0)(4.2\text{K}) = (\Delta\rho/\rho_0)_{\text{imp}}$.

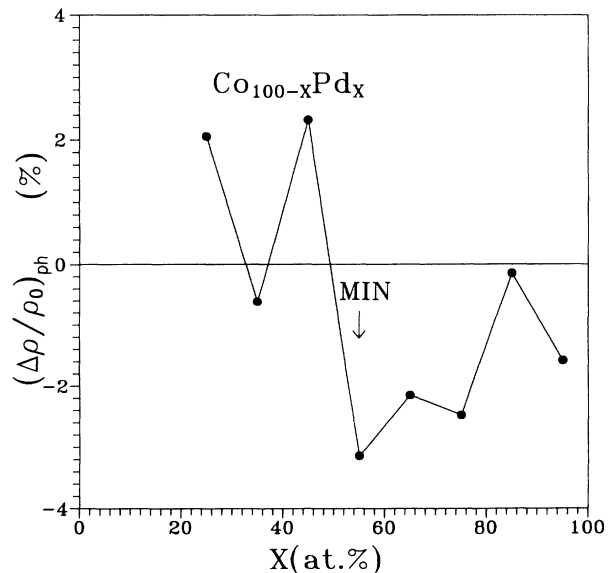


FIG. 4. $(\Delta\rho/\rho_0)_{\text{ph}}$ vs Pd concentration x .

The $(\Delta\rho/\rho_0)_{\text{imp}}$ of $\text{Co}_{100-x}\text{Pd}_x$ alloys is displayed as a function of the Pd concentration x in Fig. 3. From this picture we can see that there exists a maximum of $(\Delta\rho/\rho_0)_{\text{imp}}$ at $x \approx 55$ at. % Pd. A detailed discussion about $(\Delta\rho/\rho_0)_{\text{imp}}$ will be given in the next section. At present, we show that $(\Delta\rho/\rho_0)_{\text{ph}}$ data as a function of x in Fig. 4. Besides the irregular datum point at $x = 40$ at. %, the general trend in Fig. 4 is clear: (i) For small x , $(\Delta\rho/\rho_0)_{\text{ph}}$ is positive; (ii) as x increases, $(\Delta\rho/\rho_0)_{\text{ph}}$ becomes negative; and (iii) $(\Delta\rho/\rho_0)_{\text{ph}}$ has a minimum near $x = 55$ at. % Pd, which looks like an inverted mirror image of $(\Delta\rho/\rho_0)_{\text{imp}}$ in Fig. 3. The theoretical explanation, based on the idea of resistivity saturation of ρ^\dagger , is given in Ref. 7 to account for this phenomenon.

IV. ρ^\dagger AND ρ^\downarrow OF Co-Pd ALLOYS

The idea of the two-current model can also be used to write the residual resistivity ρ_0 of the alloy as

$$\rho_0^{-1} = (\rho^\downarrow)^{-1} + (\rho^\uparrow)^{-1}. \quad (4)$$

Then, by combining Eqs. (1) and (4), it is easy to calculate ρ^\downarrow and ρ^\uparrow , respectively, for each alloy, provided that γ is known.

As stated before, γ is determined experimentally, and it is difficult to compare it with theoretical values.¹ For example, it is estimated that $\gamma \approx 0.01$ for Ni alloys and $\gamma \approx 0.018$ for Fe alloys.⁴ Here we can use only one set of known $\Delta\rho/\rho_0$ and α data of $\text{Co}_5\text{Pd}_{95}$ to evaluate γ ; i.e., we tentatively assume that Eq. (1) is applicable to $\text{Co}_5\text{Pd}_{95}$. Then, by substituting $\Delta\rho/\rho_0 = 1.80\%$ and $\alpha \approx 2$ into Eq. (1), we find $\gamma \approx 0.018$ for Co-Pd alloys. On the other hand, it is known from the magnetization data⁵ of Co-Pd alloys that when $x \geq 75$ at. % Pd, a magnetic weakness occurs. Obviously, as x becomes large enough, ρ_{sd}^\uparrow is finite and nonzero. Then it may not be correct to use Eq. (1). We may want to use Eq. (2) instead. Before employing Eq. (2) to extract γ from the $\text{Co}_5\text{Pd}_{95}$ data, we make the following assumptions:

$$\begin{aligned} \rho^\downarrow &= \rho_{ss}^\downarrow + \rho_{sd}^\downarrow, \\ \rho^\uparrow &= \rho_{ss}^\uparrow + \rho_{sd}^\uparrow, \\ \rho_{ss}^\uparrow &= \rho_{ss}^\downarrow = \rho_{ss}. \end{aligned} \quad (5)$$

TABLE I. Magnetoresistance $\Delta\rho/\rho_0$ and residual resistivity ρ_0 at 4 K for the $\text{Co}_{100-x}\text{Pd}_x$ alloys and ρ^\downarrow and ρ^\uparrow calculated.

| Sample | $\Delta\rho/\rho_0$ (%) | ρ_0 ($\mu\Omega$ cm) | ρ^\downarrow ($\mu\Omega$ cm) ($\gamma=0.018$) ^a | ρ^\uparrow ($\mu\Omega$ cm) | ρ^\downarrow ($\mu\Omega$ cm) ($\gamma=0.036$) ^b | ρ^\uparrow ($\mu\Omega$ cm) |
|--------------------------------|----------------------------|-------------------------------|---|--------------------------------------|---|--------------------------------------|
| $\text{Co}_5\text{Pd}_{95}$ | 1.80 | 6.91 | 20.73 | 10.37 | 20.73 | 10.37 |
| $\text{Co}_{15}\text{Pd}_{85}$ | 3.90 | 15.28 | 63.67 | 20.11 | 56.54 | 20.94 |
| $\text{Co}_{25}\text{Pd}_{75}$ | 6.73 | 14.68 | 84.25 | 17.78 | 67.38 | 18.77 |
| $\text{Co}_{35}\text{Pd}_{65}$ | 7.72 | 14.25 | 89.62 | 16.94 | 69.64 | 17.92 |
| $\text{Co}_{45}\text{Pd}_{55}$ | 7.96 | 12.49 | 80.21 | 14.79 | 61.95 | 15.64 |
| $\text{Co}_{55}\text{Pd}_{45}$ | 7.51 | 11.02 | 68.02 | 13.17 | 53.23 | 13.90 |
| $\text{Co}_{65}\text{Pd}_{35}$ | 7.52 | 9.89 | 51.21 | 12.26 | 47.77 | 12.47 |
| $\text{Co}_{75}\text{Pd}_{25}$ | 6.32 | 6.78 | 37.86 | 8.39 | 30.69 | 8.85 |

^a γ is defined from $\Delta\rho/\rho_0 = \gamma(\alpha - 1)$, where $\alpha = \rho^\downarrow/\rho^\uparrow$.

^b γ is defined from $\Delta\rho/\rho_0 = \gamma(\alpha - 1)^2/\alpha$.

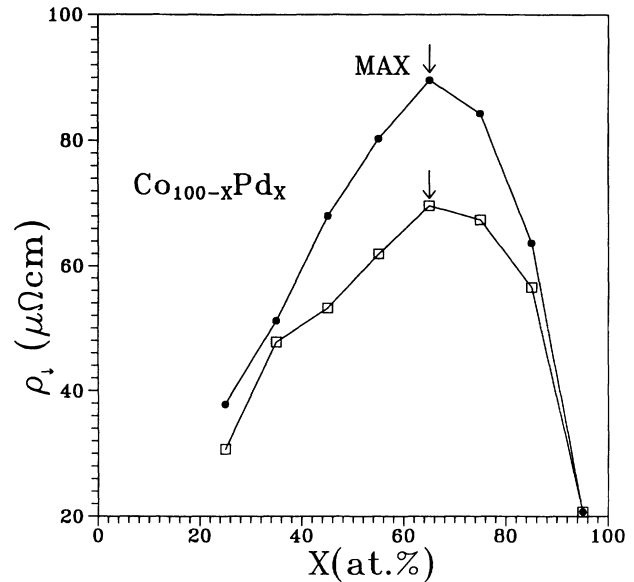


FIG. 5. Pd concentration x dependence of the spin-down resistivity ρ^\downarrow of Co-Pd alloys. The solid circles are data obtained from Eqs. (1) and (4), and the open squares are from Eqs. (4) and (6).

By substituting Eq. (5) into Eq. (2), a simpler equation is obtained:

$$\Delta\rho/\rho_0 = \gamma(\alpha - 1)^2/\alpha. \quad (6)$$

Hence, if Eq. (6) is used instead of Eq. (1), γ would turn out to be 0.036.

Having found γ , we may calculate ρ^\downarrow and ρ^\uparrow from $\Delta\rho/\rho_0$ and ρ_0 with either Eqs. (4) and (6) or Eqs. (1) and (4). Table I summarizes all the ρ^\downarrow and ρ^\uparrow values for each $\text{Co}_{100-x}\text{Pd}_x$ sample. If we plot ρ^\downarrow as a function of Pd concentration x , the result is shown in Fig. 5. There are two sets of data in Fig. 5: The solid circles are ρ^\downarrow data with $\gamma = 0.018$ and Eq. (1), and the open squares are that with $\gamma = 0.036$ and Eq. (6). Two conclusions can be made from Fig. 5: (i) A maximum of ρ^\downarrow is located at $\bar{x} = 65$ at. % Pd. This is true, irrespective of which data plot is considered. (ii) The value of maximum ρ^\downarrow is about 70 or

90 $\mu\Omega$ cm, depending on which set of data is used.

Discussions about the existence of a maximum for ρ^\downarrow and the shifting of the maximum from $x=50$ at. % are the main subject in Ref. 4. In short, Ref. 4 stresses the fact that if the scattering potential associated with alloy disorder is strong enough to cause a variation of the $3d$ wave function between chemically different atoms, d - d scattering is strong and resonant. In turn, Nordheim's rule is not obeyed for ρ^\downarrow , and a shifted maximum is observed in ρ^\downarrow . To consider Co-Pd alloys, first, the valence difference $|Z|$ between Co and Pd is 1. Therefore the split-band limit⁹ is as marginal for Co-Pd as for Co-Ni. Second, from neutron-diffraction data,¹⁰ magnetic moments $\mu_{\text{Pd}}=0.43\mu_B$ and $\mu_{\text{Co}}=1.97\mu_B$, where μ_B is the Bohr magneton. Then, according to Ref. 4, $r_s \equiv \mu_{\text{Co}}/\mu_{\text{Pd}}=4.58$, which is pretty large and indicates a strong scattering potential. Hence the case of shifted maximum in ρ^\downarrow is expected. Indeed, that is observed for Co-Pd. Another parameter of the theory is r_F , which is related to the \bar{x} location of the maximum in ρ^\downarrow by $(1-\bar{x})=(1+r_F)^{-1}$. From Fig. 5, obviously, $\bar{x}=0.65$. Then it is easy to show $r_F=1.9$ for Co-Pd. This value is the same as that for Co-Ni.

V. ρ_{ss} OF Co-Pd ALLOYS

Since it is assumed that there is no exchange splitting between the spin-up and -down s bands, $\rho_{ss}^\uparrow=\rho_{ss}^\downarrow=\rho_{ss}$, as shown in Eq. (5). However, though we do not distinguish between ρ_{ss}^\uparrow and ρ_{ss}^\downarrow , when ρ_{ss} is mentioned here, we take it to mean ρ_{ss}^\uparrow .

From Table I it is seen that ρ^\uparrow is not very different from ρ_0 . This is understood from Eq. (4), that since $\rho^\downarrow > \rho^\uparrow$, ρ_0 approximates ρ^\uparrow more than ρ^\downarrow . If $\rho^\downarrow \gg \rho^\uparrow$, as in the case of Co-Ni, it is also certain that $\rho_0 \approx \rho^\uparrow$. In Fig. 6 we have plotted the ρ_0 (solid circles) data as a function of Ni concentration x for Co-Ni. Then it is known that

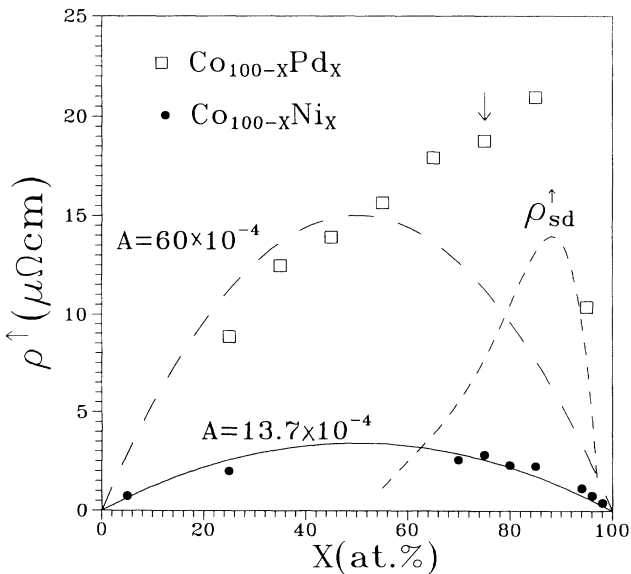


FIG. 6. Spin-up resistivity ρ^\uparrow of Co-Pd and Co-Ni alloys plotted vs the Pd or Ni concentration x .

(i) Co-Ni is a strong ferromagnet for all x , and (ii) the ρ_{ss} of the $4s$ band follows Nordheim's rule^{4,11} $\rho_{ss} \propto x(1-x)$. We use the equation

$$\rho_{ss} = Ax(1-x) \quad (7)$$

to fit all the Co-Ni data in Fig. 6. A in Eq. (7) is taken as a fitting parameter. For Co-Ni, $A = 13.7 \times 10^{-4} \mu\Omega$ cm.

For Co-Pd, we have used the ρ^\uparrow data (open squares) in the fourth column of Table I to plot Fig. 6. It is to be noted that whether the third or the fourth column of Table I was used does not make much difference.

Since it is considered that (i) Co-Pd becomes weak ferromagnetic when $x \geq 75$ at. % Pd and (ii) the ρ_{ss} of the $5s$ band still abides by the Nordheim's rule, we take the following steps to analyze our data.

The long-dashed line in Fig. 6 represents the experimental fit to Eq. (7), using $x = 25, 35, 45, 55$ at. % Pd data. A is found to be $60 \times 10^{-4} \mu\Omega$ cm. From our assumptions (i) and (ii) just mentioned and Eq. (5), ρ_{sd}^\uparrow can be estimated and is shown by the short-dashed line in Fig. 6. Because there exists some degree of arbitrariness in the fitting procedure, the set point x_{set} for ρ_{sd}^\uparrow not being equal to zero, $x_{\text{set}} \approx 50$ at. % Pd, cannot be taken too seriously. The downward arrow in Fig. 6 indicates the set point of magnetic weakness x_w , as implied from the magnetization data. It is seen that x_w differs from x_{set} . However, x_w lies in the region where ρ_{sd}^\uparrow bends up considerably. The location of maximum ρ_{sd}^\uparrow is near $x = 85$ at. % Pd, which is the same maximum as viewed from ρ^\uparrow .⁵

From the previous discussions, we have $\rho_{sd}^\uparrow \approx \rho_{ss}$ in Co-Pd. Therefore $\rho^\downarrow > \rho_{ss}$ or ρ_{sd}^\downarrow . From Eq. (5) we may further state that $\rho_{sd}^\downarrow > \rho_{sd}^\uparrow$, and ρ_{ss}^\downarrow follows Nordheim's rule also. Therefore, even if we had subtracted the ρ_{ss} contribution from ρ^\downarrow , the discussions of Sec. IV would be expected to be ρ_{sd}^\downarrow , except when ρ_{sd}^\downarrow is slightly smaller than ρ^\downarrow .

From fittings to Eq. (7), it is found that A for Co-Pd is 4.38 times larger than that for Co-Ni. Then we can make the following estimates. From theory⁴ it is known that

$$\rho_{ss}^\uparrow = \frac{m_s}{n_s e^2} D_1^s(\epsilon_F) x(1-x) \frac{1}{\tau_{ss}}, \quad (8)$$

where m_s is the electron effective mass, n_s is the number of carriers per unit volume, e is the electron's charge, $D_1^s(\epsilon_F)$ is the density of states of the spin-up s band, and τ_{ss} is the electron's relaxation time for s - s scattering. τ_{ss} can be expressed as

$$\tau_{ss}^{-1} = 2\pi \int_0^\pi (1 - \cos\theta) P(\theta) \sin\theta d\theta, \quad (9)$$

where θ is the angle between the wave vectors \mathbf{k} and \mathbf{k}' of a free electron and $P(\theta)$ is the differential scattering cross section per unit solid angle. In the approach of Mott and Jones,¹² using the screened Coulomb potential

$$V_{\text{Co-Pd}} = V_{\text{Co}} - V_{\text{Pd}} = (\Delta Z e^2 / r) e^{-qr},$$

where ΔZ is the nuclear-charge difference between Co and Pd and $1/q$ is the screening length, $P(\theta)$ is calculated to be

$$P(\theta) = \left[\frac{2m_s \Delta Z e}{\hbar^2} \right]^2 \frac{1}{[q + 4k^2 \sin^2(\frac{1}{2}\theta)]^2}. \quad (10)$$

Then

$$\tau_{ss}^{-1} = \frac{\pi}{2} \frac{(\Delta Z)^2 e^4}{\epsilon_F^2} \left[\ln \left[1 + \frac{4k_F^2}{q^2} \right] - \left[1 + \frac{q^2}{4k_F^2} \right]^{-1} \right], \quad (11)$$

where ϵ_F is the Fermi energy and k_F is the Fermi wave vector. Alternatively, the approach of de Casteljau and Friedel¹³ gives

$$\tau_{ss}^{-1} \propto \sum (L+1) \sin^2(\eta_L - \eta_{L+1}),$$

where L is the angular momentum and η_L is the phase shift. If only one η_L dominates, $\tau_{ss}^{-1} \propto \sin^2(\Delta Z \pi / 4L + 2)$. Though the result of de Casteljau and Friedel agrees with the experimental data better, the determination of phase shifts is, in general, a more complicated problem. Here we take the $(\Delta Z)^2$ form of Eq. (11) of Mott and Jones for the purpose of discussion. First, n_s , ϵ_F , q , k_F , and $D_{\uparrow}^s(\epsilon_F)$ are assumed to be roughly constants for both Co-Ni and Co-Pd. Combining Eqs. (7), (8), and (11), we obtain $A \propto (\Delta Z)^2$. For Co-Ni, $|\Delta Z| = 1$. However, for Co-Pd, because the shielding of electrons on nuclear charges is less effective and the Born approximation is less valid, its effective $|\Delta Z|$ may not be equal to the valence difference $|Z|$ exactly and may become larger than 1. The experimental data of Sec. V show that $A(\text{Co-Pd})/A(\text{Co-Ni}) \simeq 4.38$. In turn, $|\Delta Z|$ for Co-Pd appears to be about 2.09.

Strictly speaking, n_s , ϵ_F , q , k_F , and $D_{\uparrow}^s(\epsilon_F)$ may show different values and may be x dependent for $\text{Co}_{100-x}\text{Ni}_x$ and $\text{Co}_{100-x}\text{Pd}_x$. However, we are going to show that these variations are small. For example, considering the free-electron model $\epsilon_F \propto n_s^{2/3}$, $D_{\uparrow}^s(\epsilon_F) \propto n_s^{1/3} V$, and the term

$$[\ln(1 + 4k_F^2/q^2) - (1 + q^2/4k_F^2)^{-1}] \simeq \frac{1}{2},$$

in Eq. (11). Then $A \propto V(n_s)^{-2} \propto a_0^3$, where a_0 is the lattice constant of the alloy. Here $N \equiv Vn_s = (0.54e/\text{atom})$ (4 atoms/cell) for the strong ferromagnets Co-Ni and Co-Pd. Since, in general, the a_0 of Co-Pd is slightly larger than that of Co-Ni, the A of Co-Pd is larger. Using the data $a_0 = 3.86 \text{ \AA}$ ($\text{Co}_{25}\text{Pd}_{75}$) and $a_0 = 3.55 \text{ \AA}$ ($\text{Co}_{25}\text{Ni}_{75}$), we also find A to be increased by a factor of 1.28 going from Co-Ni to Co-Pd. However, this is only a minor reason to explain the change observed in A . We believe the main cause for the change still comes from the variation of $|\Delta Z|$, due to less effective shielding in Co-Pd. Hence, if the effect of a_0 has been taken into account, by setting the ratio $A(\text{Co-Pd})/A(\text{Co-Ni}) \simeq 4.38/1.28$, then $|\Delta Z|$ for Co-Pd becomes 1.85, which is a more reasonable value.

VI. CONCLUSIONS

Some magnetoresistance and electrical-resistivity data of Co-Pd alloys are reported in this study. Based on the two-current model and later extended theories, we are able to analyze ρ^{\downarrow} and ρ^{\uparrow} as a function of the Pd concentration x . For $x \geq 50-75$ at. % Pd, the spin-up and d band is not full, and $\rho_{sd}^{\downarrow} \neq 0$.

$(\Delta\rho/\rho_0)_{\text{imp}}$ and $(\Delta\rho/\rho_0)_{\text{ph}}$ are obtained by the application of Matthiessen's rule to $\Delta\rho/\rho_0$. The location in x of the maximum of $(\Delta\rho/\rho_0)_{\text{imp}}$ is the same as that of the minimum of $(\Delta\rho/\rho_0)_{\text{ph}}$.

ρ_{ss} is known to obey Nordheim's rule. ρ_{ss} increases considerably from Co-Ni to Co-Pd and then from Co-Pd to Co-Pt,¹⁴ while ρ^{\downarrow} or ρ_{sd}^{\downarrow} does not increase as much in the corresponding case. Therefore the value of $\Delta\rho/\rho_0$ decreases substantially, going from Co-Ni to Co-Pt.

ACKNOWLEDGMENTS

I am grateful to T. P. Chen for performing some experimental measurements. This work is supported by the National Science Council of ROC under Grant No. NSC80-0208-M001-85.

*Present address: Dept. of Physics, Queens College, CUNY, Flushing, NY 11367-1597.

¹I. A. Campbell, A. Fert, and O. Jaoul, *J. Phys. C. Suppl.* **1**, S95 (1970).

²O. Jaoul, I. A. Campbell, and A. Fert, *J. Magn. Magn. Mater.* **5**, 23 (1977).

³A. P. Malozemoff, *Phys. Rev. B* **32**, 6080 (1985).

⁴L. Berger, *J. Appl. Phys.* **67**, 5549 (1990).

⁵S. U. Jen, T. P. Chen, and S. A. Chang, *J. Appl. Phys.* **70**, 5831 (1991).

⁶A. B. Kaiser and S. Doniach, *Int. J. Magn.* **1**, 11 (1970).

⁷L. Berger, P. P. Freitas, J. D. Warner, and J. E. Schmidt, *J.*

Appl. Phys. **64**, 5459 (1988).

⁸R. Parker, *Proc. Phys. Soc. London A* **64**, 447 (1951).

⁹L. Berger, *Physica* **91B**, 31 (1977).

¹⁰J. W. Cable, E. O. Wallan, and W. C. Koeller, *Phys. Rev.* **138**, A755 (1965).

¹¹L. Nordheim, *Ann. Phys. (N.Y.)* **9**, 607 (1931).

¹²N. F. Mott and H. Jones, *The Theory of the Properties of Metals and Alloys* (Oxford University Press, Oxford, 1936).

¹³P. de Faget de Casteljau and J. Friedel, *J. Phys. Radiat.* **17**, 27 (1956).

¹⁴S. U. Jen and T. P. Chen (unpublished).